

To be submitted to  
Annali di Radioprotezione

ISTITUTO NAZIONALE DI FISICA NUCLEARE  
Laboratori Nazionali di Frascati

LNF-83/14(P)  
14 Marzo 1983

A. Esposito and M. Pelliccioni: RADIATION PROTECTION  
MEASUREMENTS AROUND THE NEW POSITRON  
CONVERTER TARGET

INFN - Laboratori Nazionali di Frascati  
Servizio Documentazione

LNF-83/14(P)  
14 Marzo 1983

## RADIATION PROTECTION MEASUREMENTS AROUND THE NEW POSITRON CONVERTER TARGET

A. Esposito and M. Pelliccioni  
INFN - Laboratori Nazionali di Frascati, Frascati, Italy.

### 1. - INTRODUCTION.

The Linac of LNF is composed of 12 accelerating sections where the electron or the positrons can be accelerated up to an energy of about 400 MeV. In the first high intensity section, i. e. in the first 4 accelerating sections, electrons can be accelerated up to about 70 MeV reaching intensities up to 400 mA. At that point of the beam line an electron-to-positron converter can be introduced. For the experiments with the positron beam, the converter consists of a high duty cycle target. In the past this target was a copper cylinder 13 mm thick. Since two years, a new more efficient target made of 1 mm copper and 5 mm gold has been installed.

In the second part of the Linac the electrons or the positrons are either accelerated to the maximum energy and directed toward the experimental facilities (Leale) or accelerated to about 300 MeV and injected into the storage ring. The pulse length can be varied between about 0.01  $\mu$ s and 4  $\mu$ s; repetition rates up to 200 Hz can be achieved. The maximum currents available at the upper energies are 100 mA for  $e^-$  and 500  $\mu$ A for  $e^+$ .

In this note the results of several radiation protection measurements are reported, concerning machine operation with the new converter target.

## 2. - DOSE RATES AROUND THE CONVERTER DURING MACHINE OPERATION.

As it is well known, when a high-energy electron beam strikes a thick target, a large part of the energy is converted into bremsstrahlung X-rays which constitute, by far, the major component of the secondary radiation produced. The emission of these X-rays depends on a number of factors such as power loss, electron energy, thickness and material of the target, angle of emission. Experimental results of dose-rate measurements versus angle and target depth in the energy range between 20 and 100 MeV with electron beams incident on thick targets have been summarized by Wyckoff et al.<sup>(1)</sup>. On the base of these and other experimental results, an empirical law relating the different parameters has been determined<sup>(2)</sup>.

We have measured the dose rates in various directions around our linac converter. The experimental layout is shown in Fig. 1. Since the converter is almost completely shielded as close as possible by lead bricks 5 cm thick, the measurements have been made outside the shield.

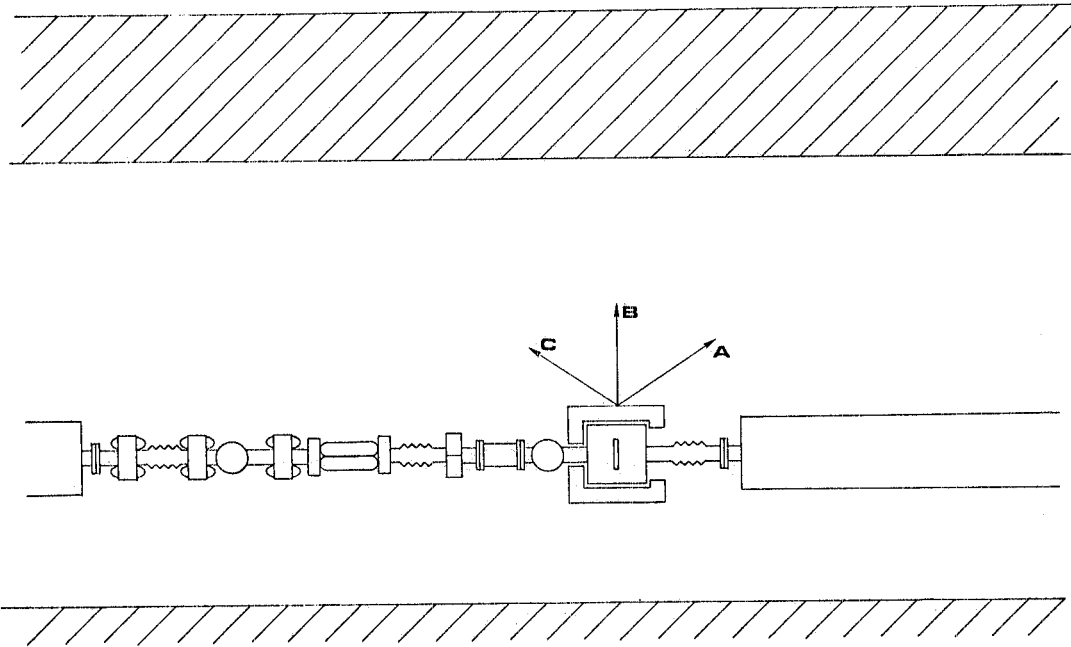


FIG. 1 - Experimental layout.

The power of the electron beam striking the target was about 4.5 kW ( $E = 70$  MeV;  $I_p = 160$  mA;  $\tau = 4 \mu\text{s}$ ;  $\nu = 100$  Hz). The measurements have been made by thermoluminescence dosimeters (Harshaw Model 4040 TL bulb dosimeters  $\text{CaF}_2:\text{Mn}$ ) and the results are shown in Fig. 2. Letters A, B, C refer to the three directions indicated in Fig. 1. Distances are measured from the lead screen surrounding the converter.

Some irregularities in the curves shown in Fig. 2 are due to the presence of fortuitous shields or to possible gaps in the lead screen (i. e. for the curve B). However, the results reflect the correct orders of magnitude for the quantities of interest.

Taking into account the attenuation produced by the 5 cm thick lead shield and other materials surrounding the target, a reasonable agreement can be found with data from the literature. The trend of dose rate versus distance, however, does not seem to follow the inverse square law as predicted, probably because of a diffuse background due to other source points.

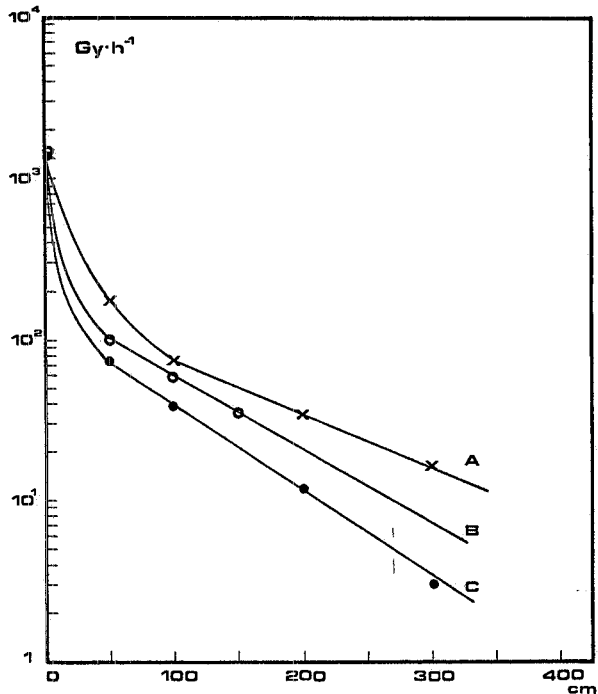


FIG. 2 - Dose rates vs distance from the converter for 4.5 kW of the electron beam striking the target.

### 3. - INDUCED RADIOACTIVITY IN MACHINE STRUCTURES.

Because of the high power dissipated inside the converter, the latter and the machine parts close to it become intensely activated. Most of the induced activity is due to reactions of type  $(\gamma, n)$  in the metallic structures. A study of the various possible reactions and estimations of the expected induced activity levels along the linac guide have been performed some time ago<sup>(3)</sup>.

A gamma energy spectrum has been obtained recently in the region close to the converter by means of an intrinsic germanium crystal. Peaks corresponding to  $^{46}\text{Sc}$ ,  $^{54}\text{Mn}$ ,  $^{57}\text{Co}$ ,  $^{58}\text{Co}$ ,  $^{59}\text{Fe}$ ,  $^{60}\text{Co}$ ,  $^{65}\text{Zn}$ ,  $^{124}\text{Sb}$ , have been identified, in addition to the 511 keV peak of  $\beta^+$  emitters.

Activation of structural materials presents a relevant exposure risk when performing maintenance work. Among the most important interventions in this respect we mention the periodical replacement of the converter target. This operation takes place as a rule every  $2-3 \times 10^8$  pulses because of radiation damage effects. The latters show up as a crater with indented edges, the gold being expelled as minute particles. It is not yet clear by which physical process such a cavity is formed<sup>(4)</sup>.

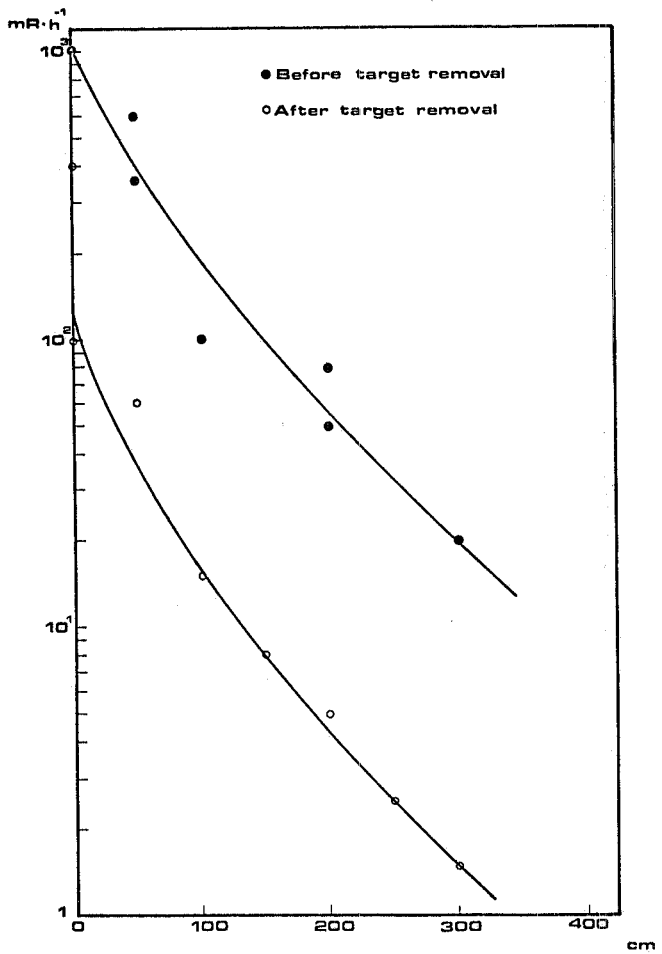


FIG. 3 - Radiation levels measured by a portable monitor around the converter.

The radiation levels measured by a portable monitor when performing one such intervention are shown in Fig. 3. Values obtained before target replacement refer to measurements taking place about 36 hours after machine stop outside the lead shield surrounding the converter. The other values were measured at the end of the intervention, namely in this case removal of both the target and the positron lens. Sometimes different exposure rates were measured in different directions, the distance being the same. That can be explained by some irregularities in the converter shield.

The above operation took place after  $7.145 \times 10^7$  pulses incident on the target ( $E = 70$  MeV,  $I_p = 170$  mA,  $\tau = 4\mu s$ ;  $v = 100$  Hz). Exposure rate measured as close as possible to the removed target by means of a portable monitor was about 10 R/h.

A spectral analysis of gold filings from another target, made by an intrinsic germanium crystal several months after the target had been removed, showed the presence of  $^{195}\text{Au}$ ,  $^{60}\text{Co}$ ,  $^{57}\text{Co}$  and  $^{125}\text{Sb}$ . The latest is likely however to stem from the nearby lead shield containing precisely 5% antimony.

It is worth noting, finally, that in one occasion when the lead shield surrounding the converter was dismantled, up to 40 R/h were measured with a portable monitor located as close as possible to the accelerator guide.

#### 4. - INDUCED ACTIVITY IN THE AIR.

As it is known, radioactive gases can be produced in the air surrounding a power accelerator. The most important are  $^{13}\text{N}$  ( $T_{1/2} \approx 10$  min) and  $^{15}\text{O}$  ( $T_{1/2} \approx 2$  min). They are  $\beta^+$  emitters originating from  $(\gamma, n)$  reactions in air nitrogen and oxygen.

Concerning the LNF linac, expected concentrations were estimated in the past<sup>(5)</sup>

and recently some measurements were published<sup>(6)</sup>. We want to report here some further measurements concerning linac operation with the electron beam hitting the converter.

These measurements have been made both inside the chimney stack near the exit of the ventilation duct, and at various distances from it in order to study the effect of atmospheric dilution. To that purpose, air was pumped through a chamber with plastic scintillator-coated walls by an aspirator provided with a dust filter. The results of the measurements are shown in Fig. 4, where the radioactive gas concentrations

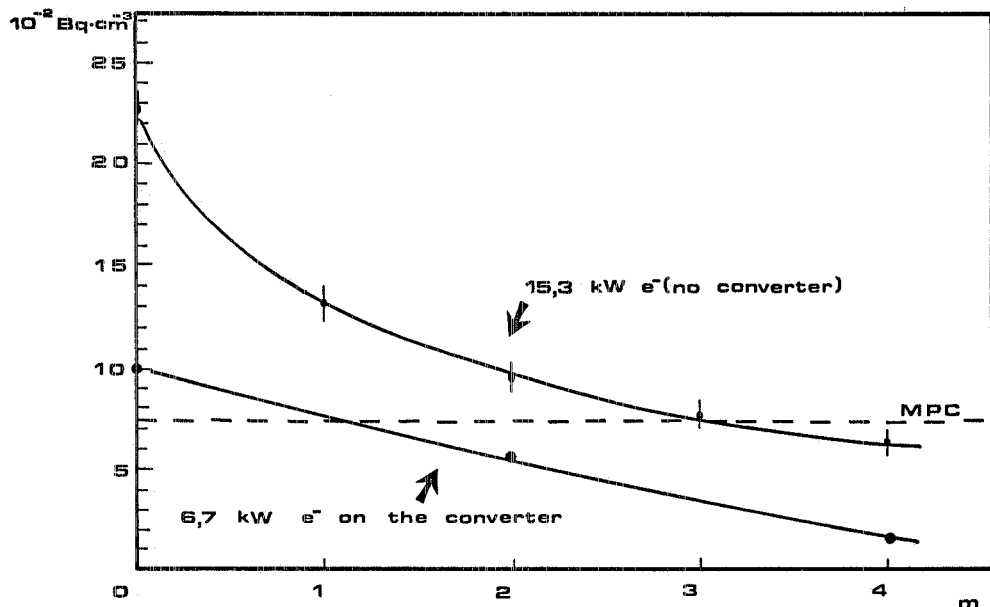


FIG. 4 - Radioactive gas concentrations vs distance from the exhaust duct mouth.

are displayed versus distance from the exhaust duct mouth. Another curve in the same figure concerns accelerator operation without the converter target being inserted. It should be noted that in such conditions the concentration of radioactive gases depends strongly on beam losses. The curve shown should then be regarded only as an example, the specific case being probably one of very high losses.

In both cases referred to in Fig. 4, the measured concentrations at the exhaust vent happen to be higher than the maximum permissible concentrations (about  $7.4 \times 10^{-2} \text{ Bq}/\text{cm}^3$ )<sup>(7)</sup>. Such a vent, however, is located on the roof of a building which is normally inaccessible even for the Centre staff. In addition, the machine operates in those conditions only for a small percent of the total running time. When injecting into the storage ring, in fact, the accelerator power is 100 times smaller and no appreciable

radioactive gas concentration can be measured at the ventilation exit mouth.

Besides, it has been calculated, under beyond any doubt conservative assumptions, that a release of  $10^7$  Bq/s, i. e.  $2.6 \times 10^{14}$  Bq/y ( $\approx 7000$  Ci/y), would produce an average dose rate of  $2.5 \mu\text{Sv}/\text{h}$  ( $0.25$  mrem/h) at 20 m from the release point<sup>(8)</sup>.

In our case, taking into account the speed of air release from the linac ventilation circuit and the flow rate, the activity release rate corresponding to the operating conditions of Fig. 4 would be of the order of  $10^5$  Bq/s. The dose rate at 20 m from the release point would then be at most  $2.5 \times 10^{-2} \mu\text{Sv}/\text{h}$  ( $2.5 \mu\text{rem}/\text{h}$ ).

In order to identify the component nuclides in the radioactive gas mixture, we studied its decay in some samples of activated air. One of the so established decay curves is shown in Fig. 5. From the different half-lives it was so possible to infer the presence of  $^{15}\text{O}$ ,  $^{13}\text{N}$  and, although in smaller concentration, of  $^{38}\text{Cl}$  ( $T_{1/2} \approx 37.3$  min). No evidence was found for  $^{11}\text{C}$ , which yet should to be expected, probably because it was produced in a much smaller concentration than the other gases.

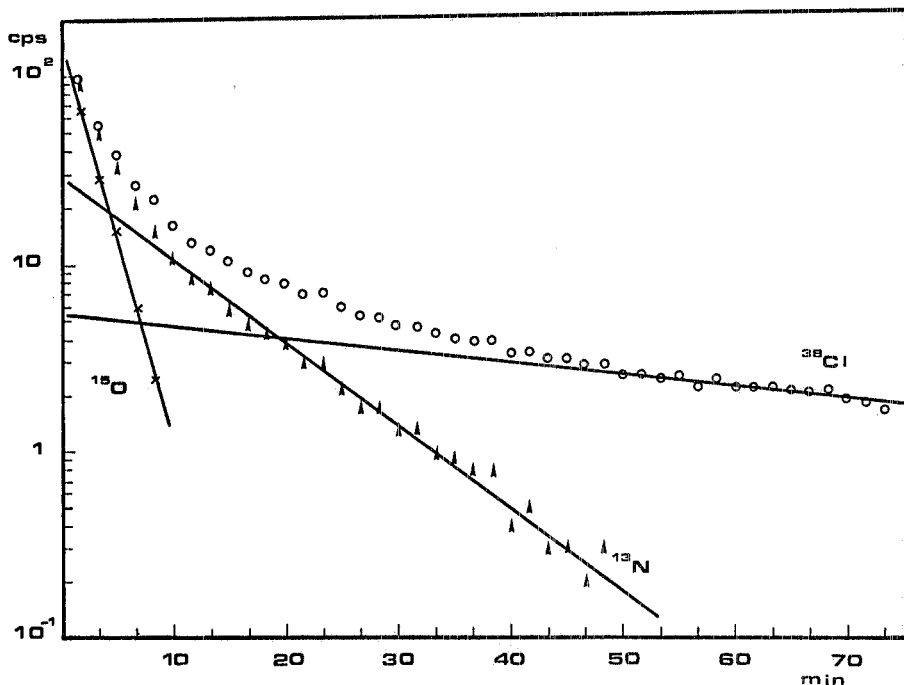


FIG. 5 - Decay curve of an activated air sample.

For what concerns operational physical surveillance, it is worth noting explicitly that exposure takes place in this case essentially via submersion rather than by intake. Derived Air Concentrations were in fact evaluated according to the effect of external irradiation by 0.511 MeV positron annihilation gamma rays. Instruments normally

used for external radiation monitoring may then still be employed. By a set of thermo-luminescence dosimeters installed at the exit of the linac ventilation stack, an average dose of  $25 \mu\text{Gy}$  (2.5 mrad) was measured, corresponding to  $1.53 \times 10^7$  pulses of a 5 kW electron beam incident on the converter target. Such a dose corresponds to a rate of about  $0.6 \mu\text{Gy/h}$  (0.06 mrad/h), about half of which, however, is due to environmental background, as shown by in loco measurements made with a high-pressure ionization chamber (Reuter Stokes mod. RS111).

A systematic dose surveillance at the stack exit is implemented by means of TLD and gamma film-badges. The highest measured annual dose was up to now 2.29 mSv (229 mrem) background included.

At the same location, inside the ventilation stack near the exit mouth, we tried eventually to measure ozone concentration during machine operation by means of a Dasibi analyzer mod. 1003 AH. No appreciable concentration, however, could be measured above background level (0.012 ppm).

#### 5. - INDUCED ACTIVITY IN COOLING WATER.

Cooling water can become activated as well. Radionuclides most likely to be formed are again  $^{13}\text{N}$  and  $^{15}\text{O}$ . However, water samples taken from the cooling circuit of the converter target contain as a rule also a large number of radionuclides whose origin is corrosion of machine metallic structures. Table I shows as an example the re-

TABLE I - Results of a  $\gamma$ -ray spectrometry of a water sample from the converter target cooling circuit.

Radionuclide	$T_{1/2}$	Activity measured	
		Bq	Bq/cm <sup>3</sup>
$^{58}\text{Co}$	70.78 d	23.9	0.612
$^{65}\text{Zn}$	244.1 d	22.5	0.577
$^{57}\text{Co}$	271.4 d	5.64	0.140
$^{60}\text{Co}$	5.272 y	2.25	0.058
$^7\text{Be}$	53.3 d	2.07	0.053
$^{54}\text{Mn}$	312.3 d	0.4	0.010
$^{199}\text{Au}$	3.13 d	traces	

sults of a spectral analysis made two days after sampling by means of an intrinsic germanium crystal spectrometer.

It can be observed that all identified radionuclides ( $^{7}\text{Be}$  excepted) are corrosion products from activated metals who are at some time becoming in contact with cooling water. On the other hand, all  $\beta^+$  emitters directly produced in water are missing from the table: this should not be surprising, as they had certainly disappeared at the time of counting because of their short half life.

A water sample from the same circuit has also been analyzed at the Environmental Science Laboratory of ENEA (C. S. N. Casaccia) in order to assess the tritium content. Its concentration turned out to be by far larger than that of gamma emitters (3.7 Bq/ml).

#### 6. - INDUCED RADIOACTIVITY IN DUST.

We report eventually about measurements performed on dust samples from the linac tunnel floor close to the converter. Also in this case the radionuclides which are usually identified come from corrosion of activated metals in the machine and of other installed equipment.

The radionuclide type and amount show in general a wide range of variation according to the kind of operation being performed. A typical example of results from a spectral analysis by means of the above mentioned intrinsic germanium spectrometer is shown in Table II. It refers to a 0.446 g dust sample collected over a surface of about  $3000 \text{ cm}^2$ . In the last column are reported the surface contamination derived limits for controlled areas as recently re-calculated by NRPB, taking into account the most recent informations about possible exposure pathways and the dose limits recommended by ICRP Publication 26<sup>(10)</sup>.

How can be observed, the measured superficial activities turn out to be always lower than the proposed derived limits. It seems wise, however, to keep this problem attentively under control. The origin of such a contamination suggests indeed that special operations could bring to an undesirable increase of it. One such case truly happened as a consequence of a converter breakdown: the rupture of the target and of the positron lens caused flooding of the container by water from the cooling circuit. On that occasion, a dust sample ( $\approx 0.072 \text{ g}$ ) was collected over about  $1000 \text{ cm}^2$  of floor surface, at the same location as the one previously discussed. The results of the analysis, performed some days after the incident, are reported in Table III.

TABLE II - Results of the  $\gamma$ -ray spectrometry of a dust sample collected from the linac tunnel floor close to the converter.

Radionuclide	$T_{1/2}$	Activity measured			Derived limits <sup>(9)</sup> $Bq/cm^2$
		Bq	Bq/g	$Bq/cm^2$	
$^{65}\text{Zn}$	244.1 d	38	81	$1.3 \times 10^{-2}$	$3 \times 10^2$
$^{58}\text{Co}$	70.78 d	5.5	12	$1.8 \times 10^{-3}$	$3 \times 10^1$
$^{57}\text{Co}$	271.4 d	3.2	7	$1.1 \times 10^{-3}$	$3 \times 10^2$
$^{60}\text{Co}$	5.272 y	1.2	2.5	$4 \times 10^{-4}$	$3 \times 10^1$
$^{54}\text{Mn}$	312.3 d	1.2	2.5	$4 \times 10^{-4}$	$3 \times 10^2$
$^{124}\text{Sb}$	60.20 d	0.8	1.8	$3 \times 10^{-4}$	$3 \times 10^1$
$^{22}\text{Na}$	2.6 y	0.5	1	$2 \times 10^{-4}$	$3 \times 10^1$
$^{56}\text{Co}$	78.5 d	0.2	0.4	$1 \times 10^{-4}$	$3 \times 10^1$

TABLE III - Results of the  $\gamma$ -ray spectrometry of a dust sample collected from the linac tunnel floor close to the converter.

Radionuclide	$T_{1/2}$	Activity measured			Derived limits <sup>(9)</sup> $Bq/cm^2$
		Bq	Bq/g	$Bq/cm^2$	
$^{57}\text{Co}$	211.4 d	310	$4.3 \times 10^3$	$3.1 \times 10^{-1}$	$3 \times 10^2$
$^{58}\text{Co}$	70.78 d	88.4	$1.2 \times 10^3$	$8.8 \times 10^{-2}$	$3 \times 10^1$
$^{196}\text{Au}$	6.18 d	81	$1.1 \times 10^3$	$8.1 \times 10^{-2}$	$3 \times 10^1$
$^{60}\text{Co}$	5.272 y	73.2	$1.0 \times 10^3$	$7.3 \times 10^{-2}$	$3 \times 10^1$
$^{198}\text{Au}$	2.695 d	55.9	$7.7 \times 10^2$	$5.6 \times 10^{-2}$	$3 \times 10^1$
$^{54}\text{Mn}$	312.3 d	11.6	$1.6 \times 10^2$	$1.2 \times 10^{-2}$	$3 \times 10^2$
$^{47}\text{Sc}$	3.4 d	1.18	$1.6 \times 10$	$1.2 \times 10^{-3}$	$3 \times 10^1$
$^{65}\text{Zn}$	244.1 d	0.04	$5.8 \times 10^{-1}$	$4 \times 10^{-5}$	$3 \times 10^2$

As can be seen, although the superficial activities are in this case larger than those in Table II, the recommended derived limits are still not exceeded. Also the radionuclide composition is different. The presence of gold radioisotopes can be noted, showing with certainty an origin from the converter target. Their importance would have been even more evident, had the measurement taken place immediately after the intervention.

The sample spectrum was showing the peak of  $^{195}\text{Au}$  too, it has not been reported in the table, however, as it was too difficult to evaluate in a quantitative way with respect to background.

The example discussed, although reflecting particular conditions, shows the need not to neglect this possible environmental pollution pathway, sometimes overlooked in accelerator radiation protection.

REFERENCES.

- (1) - J. M. Wyckoff et al., Dose versus angle and depth produced by 20 and 100 MeV electrons incident on thick targets, Proc. Conf. Protection against Accelerator and Space Radiation, CERN 1971, Report CERN 71-16 (1971), p. 773.
- (2) - A. H. Sullivan, Radiation levels expected inside the LEP preinjector tunnel, Internal Report CERN HS-RP-IR/82-50 (1982).
- (3) - M. Ladu, M. Pelliccioni e M. Roccella, Radioattività residua sulla guida d'onda del linac di Frascati, Minerva Fisico-Nucleare 11, 103 (1967).
- (4) - V. Chimenti, G. Turchetti e A. Vitali, Targhetta  $e^-e^+$  del positron converter, Memorandum Interno del 22/12/1982.
- (5) - M. Ladu, M. Pelliccioni e M. Roccella, Produzione e scarico di gas tossici e radioattivi nel tunnel del Linac di Frascati, Giornale di Fisica Sanitaria e Protezione contro le Radiazioni 11, 112 (1967).
- (6) - S. Amatiste, P. Cavallucci, A. Esposito e M. Pelliccioni, Protezione ambientale intorno all'acceleratore lineare di Frascati, Frascati Report LNF-81/4 (1981).
- (7) - C. Yamaguchi, MPC calculation for the radionuclides produced during accelerator operation, Health Phys. 29, 393 (1975).
- (8) - A. H. Sullivan, Criteria for assessing the release of radioactive air from accelerator, Internal Report CERN HS-RP-IR/82-26 (1982).
- (9) - A. D. Wrixon, G. S. Linsley, K. C. Binns and D. F. White, Derived limits for surface contamination, Harwell Report NRPB-DL2 (1979).
- (10) - ICRP Publication 26, Recommendations of the International Commission on Radiological Protection (Pergamon Press, 1977).